DESIGN OF FRESNEL HOLOGRAMS FOR OPTICAL INTERCONNECTIONS OF VLSI

H.S. Façanha, D.R. Selviah, K. Steptoe and M. Zhi-Qiang

University College London, UK

INTRODUCTION

The current interest in computer generated holograms for free-space optical interconnection of integrated circuits is driven by the need to address the limitations of high speed, high density electrical interconnects. Optical interconnection of signals offers potential advantages, as described by Goodman et al (1): different optical signals can propagate without interference, free from capacitive loading effects and transmission line dispersion.

Computer generated Fresnel holograms for optical interconnects were presented by Feldman and Guest (2). They evaluated the specific requirements of holograms for optically interconnecting VLSI and they described a sampling technique for hologram formation that uses a laser scanning system. This paper describes the design of a computer generated holographic optical element (HOE) interconnecting one-to-n optical components on the surface of a VLSI chip, through the use of an off-axis, binary hologram. We devise here a novel way of drawing the patterns that compose the hologram: instead of using the conventional sampling technique, we derive an equation which describes the analytic behaviour of the interference pattern, and approximate its elliptical shape by line segments at different angles.

DESIGN APPROACH

A hologram can be produced optically by recording the interference pattern of an object wave and a reference wave. Holograms synthesised by computer are used for constructing optical wavefronts from numerically specified objects, i.e., wavefronts from objects that do not physically exist can be created.

Calculation of the interference pattern in the hologram plane can be carried out with theories appropriate for Fraunhofer (far field) or Fresnel (near field) diffraction. In the case of the HOE for optical interconnects, where the object is in the near field, either microlenses must be inserted between the hologram and the VLSI chip to image the far field pattern or Fresnel holograms must be considered. The microlens approach relieves the lateral alignment tolerances of the hologram but it increases the angular hologram alignment tolerance and introduces an additional component which must also be aligned. So we have concentrated on the Fresnel type of holograms.

A new approach for Fresnel hologram computation is presented here, based on the analytic description of the elliptical shapes that constitute the fringes of the interference pattern. It offers several advantages over the conventional sampling technique: (a) compatibility - the data obtained is fed directly to a large dimension plotter to draw the layout. Large plotters of this type are regularly used by VLSI designers for plotting out their electronic layout and so are readily available to them. (b) compactability - sampling techniques result in large datafiles for high resolution layouts, since the image is composed of squares, all in the same orientation. The datafiles for the plotter are much smaller since lines of various lengths and widths can be drawn at various angles; (c) accuracy - plotter is a higher resolution device compared to a laser printer and large drawings can be produced. This results in a further resolution improvement after photoreduction. Smooth curves can be drawn as opposed to stepped approximations. These benefits are retained if the technique is extended to electron-beam formation and so is not limited to the resolution of the media.

Figure 1 shows the arrangement for a Fresnel hologram imaging one laser source/modulator to one detector/modulator. Extending this to include one-to-n interconnects can be made by superimposing single holograms. The next section presents the geometry analysis of the interference pattern for the Fresnel hologram.

DERIVATION OF THE FRESNEL HOLOGRAM DESIGN EQUATIONS

The interference of light emitted by two point sources P and R is described by Collier et al (3). Assume that $p = p_0 \exp(i\psi_p)$ and $r = r_0 \exp(i\psi_r)$ are the complex amplitudes of the light arriving at the hologram plane from the subject and reference point sources, respectively, and that they emanate spherical waves in phase. The irradiance I_q at any point Q in space as a function of the irradiance I_p and I_r at the point sources is given by

$$I_q = I_p + I_r + 2(I_p I_r)^{1/2} \cos\delta , \qquad .....(1)$$

with the phase difference

$$\delta = 2\pi/\lambda \, (r_r - r_p), \qquad .....(2)$$

where

λ = wavelength,

r_r (r_p) = distance from point source R(P) to point Q.

The periodic spatial variation of intensity in the interference fringes is governed by the phase difference δ and the locus of points of maximum irradiance is determined by setting $\delta = 2\pi N$, thus providing

$$r_r - r_p = N\lambda , \quad N = 0,1,2,.. \qquad .....(3)$$

This equation describes a family of hyperboloids of revolution about the axis RP connecting the two point sources. In order to compute the subject-reference phase difference consider that the subject and reference point sources P and R are in the source plane at coordinates $P = (x_p, y_p, z_p)$ and $R = (x_r, y_r, z_r)$ respectively. The origin of the system is considered to be at the hologram plane. The system is shown in Figure 1.

At a point $Q = (x,y,z=0)$ in the hologram plane the locus of points of maximum irradiance occur at

$$r_r - r_p = [(x-x_r)^2 + (y-y_r)^2 + z_r^2]^{1/2} - [(x-x_p)^2 + (y-y_p)^2 + z_p^2]^{1/2} = N\lambda. \quad .....(4)$$

This equation can be manipulated to take the form of a conic equation:

$$Ax^2 + Bxy + Cy^2 + Dx + Ey + F = 0, \quad .....(5)$$

where

$$A = 4N^2\lambda^2 - 4(x_r-x_p)^2, \quad .....(6)$$

$$B = -8(x_r-x_p)(y_r-y_p), \quad .....(7)$$

$$C = 4N^2\lambda^2 - 4(y_r-y_p)^2, \quad .....(8)$$

$$D = -4N^2\lambda^2(x_r+x_p) - 4(x_r-x_p)(x_p^2+y_p^2-x_r^2-y_r^2), \quad .....(9)$$

$$E = -4N^2\lambda^2(y_r+y_p) - 4(y_r-y_p)(x_p^2+y_p^2-x_r^2-y_r^2), \quad ....(10)$$

$$F = 4N^2\lambda^2(x_p^2+y_p^2+z_p^2) - [N^2\lambda^2 + (x_p^2+y_p^2-x_r^2-y_r^2)]^2, \quad ....(11)$$

This equation has solution in R^2 when

$$N > 1/\lambda\, [(x_r-x_p)^2+(y_r-y_p)^2+4h^2]^{1/2} \quad ....(12)$$

Applying condition (12) to equation (5) results in a set of concentric ellipses that grow with the variable N. Each ellipse is rotated by an angle θ and translated by an amount (centrex, centrey) in relation to the origin of the XY axis of the hologram. Simplification of a conic equation through the use of rotations and translations are well described by Fuller and Tarwater (4). The rotation angle and the translation components can be defined as

$$\theta = 1/2\ tg^{-1}(B/(A-C)), \quad ....(13)$$

$$centrex = -(D\cos\theta + E\sin\theta) / 2(A\cos^2\theta + B\sin\theta\cos\theta + C\sin^2\theta), \quad ....(14)$$

$$centrey = -(E\cos\theta - D\sin\theta) / 2(A\sin^2\theta - B\sin\theta\cos\theta + C\cos^2\theta). \quad ....(15)$$

The simplified ellipse, after rotation and translation, take the form

$$A'x'^2 + C'y'^2 + F' = 0, \quad ....(16)$$

or the more common representation

$$x'^2/a^2 + y'^2/b^2 = 1, \quad ....(17)$$

where

$$a^2 = -F'/A', \quad ....(18)$$

$$b^2 = -F'/C', \quad ....(19)$$

$$A' = A\cos^2\theta + B\sin\theta\cos\theta + C\sin^2\theta, \quad ....(20)$$

$$C' = A\sin^2\theta - B\sin\theta\cos\theta + C\cos^2\theta, \quad ....(21)$$

$$F' = A'centrex^2 + C'centrey^2 + (D\cos\theta + E\sin\theta)\ centrex + (E\cos\theta - D\sin\theta)\ centrey + F \quad ....(22)$$

Experiments were carried out to demonstrate the application of the above equations in generating holograms by computer and these are now described.

EXPERIMENTAL DEMONSTRATION OF THE USE OF THE DESIGN EQUATIONS WITH A PEN PLOTTER

A program was written to implement the interconnection of one laser source to a matrix of an arbitrary number of detectors (see Figure 1). It accepts as input parameters the wavelength (λ), the separation between the hologram plane and the source-detectors plane (h), the distance between the laser source and the centre of the array of detectors (dx, dy), the number of detectors in the array (xarray, yarray) and the size of the matrix grid (gridx, gridy). For each detector of the array the program generates the set of concentric ellipses that constitute its interconnection hologram. The algorithm evaluates equations (18) and (19) to obtain the ellipses dimensions and equations (13), (14) and (15) to compute their rotation angle and centre coordinates. This data is outputted to a file in the form of a set of commands to a pen plotter.

A simple test was carried out to demonstrate the behaviour of this program. For the purpose of demonstration the following parameters were employed: (a) λ = 0.6328 microns; (b) h = 5 cm; (c) dx, dy = 14 cm; (d) gridx, gridy = 4 mm. Two holographic interconnection patterns were generated: one imaging one laser source to a 2 X 2 matrix of detectors and another imaging one source to a 4 X 4 matrix. The plotter artworks were reduced 64 times using a conventional camera (with fixed reduction factor of 8) and a Kodak ortho-film. A holographic film was not used since the photographic equipment (10 microns resolution) could not meet the fine resolution required by this kind of film. After processing the negatives were exposed to a focused red Helium neon laser simulating a point source, as mentioned in reference (2), in order to obtain the focused spots generated by the holograms. A scaled plotter artwork corresponding to the hologram imaging one source to a 2 X 2 matrix of detectors is shown in Figure 2. The 4 X 4 array of light spots produced by the hologram connecting one-to-4X4 matrix can be seen in the photograph of Figure 3, verifying the validity of the equations.

APPLICATION TO VLSI CIRCUITS

The tests described in the previous section enabled us to set up a simple laboratory experiment to demonstrate our method, but they used parameters not compatible with the requirements of VLSI circuits. Application of equation (5) to typical conditions of VLSI circuits is shown in Figures 4 to 7. Figures 4 and 5 present the hologram dimensions describing the interconnection pattern of two point sources separated by a distance r ($r = (x^2 + y^2)^{1/2}$), scaled by the wavelength. The concentric ellipses that compose the hologram can be identified in the graphs by its major axis (2a), parallel to the line connecting the two point sources (r), and its minor axis (2b), perpendicular to that same line. Heights between the hologram and the source-detector plane are considered $h = 5000\lambda$ and $h = 15000\lambda$, corresponding to heights of approximately 0.4 and 1.3 cm, respectively, for a wavelength around 850 nm. These curves show the boundary of the biggest ellipse of the layout, which is the one whose fringe width (Δf) reaches the resolution of the recording medium (e-beam machine, holographic film). This resolution was considered to be $f = \lambda$ and $f = 2\lambda$.

By choosing the resolution of the recording medium (Δf) to λ or 2λ, and setting the spacing between the hologram and the source-detectors plane (h) to 5000λ or 15000λ, it is possible to use graphs 4 and 5 to find the dimensions of the hologram (a and b) for a wide range of distances (r) between the source and the detector.

Considering the typical case of a wavelength of 850 nm, a separation between the hologram and the substrate of 0.5 cm, a resolution for the recording medium of 1 micron and a separation between the source and detector of 2 cm, the values of the major and minor axis of the biggest ellipse that constitute the hologram would be 2a = 10010 microns and 2b = 4864 microns respectively. These values correspond to a number of fringes equal to 606.

The results of Figures 4 and 5 were used to draw Figures 6 and 7 representing directly the size of the spot at the detector, w_a and w_b (corresponding to the directions of the ellipse axis a and b respectively), according to the analysis presented by (5).

The first two graphs can also be used to derive other significant results, for example, determining the size of the hologram that matches the characteristics of the laser source, as defined in (2). Also, these graphs can be useful in determining how to divide the area above the integrated circuit in order to accommodate various holograms when using more than one source imaging to many detectors (space-variant system).

FUTURE WORK

It is planned to use an electron-beam machine to generate directly a mask with the interference pattern. The holographic interconnection program will be modified to drive this equipment, by drawing rectangles of various lengths and widths at various angles. This datafile can be much smaller than for a pixelated square sampling approach and a higher resolution realisation of smooth curves can be formed.

Using the e-beam technique, it is intended to generate a surface relief hologram that simulates a 4-grey-level. Since e-beam unities are binary in nature, four black and white masks will be produced. Superimposing these masks during the surface relief fabrication process is expected to produce a 4-grey-level holographic pattern.

CONCLUSION

An approach to the design of computer generated holograms for optical interconnection of integrated circuits has been described. This system is capable of producing Fresnel holograms that interconnect one laser source to a matrix of detectors, using parameters such as the wavelength, the distance between the hologram and the source-detectors planes, the separation between source and detectors, the number of detectors in the matrix and the size of the detectors grid. A feature of this approach are the equations, derived so that direct writing using e-beam techniques can be employed. This was demonstrated using artwork produced on a pen plotter and using conventional photographic techniques to photoreduce it. Finally, the application of this approach to real VLSI were explored. Design graphs showed the limiting dimensions of the hologram and the minimum spot size that it generates. In the future, it is planned to use this technique to achieve a 4-grey-level surface relief hologram for optical interconnection using an e-beam machine and angled rectangles to approximate the holographic pattern.

ACKNOWLEDGEMENTS

H. S. Facanha is sponsored by a grant from Conselho Nacional de Desenvolvimento Cientifico e Tecnologico (C.N.Pq.) of Brazil. The authors would like to acknowledge Prof. John Midwinter of the Department of Electrical and Electronic Engineering, University College London, for some useful discussions during the final stages of this work.

REFERENCES

1. Goodman, J.W. et al., 1984, "Optical Interconnections for VLSI systems", IEEE Proceedings, 72, 850-865.

2. Feldman, M.R., and Guest, C.C., 1987, "Computer Generated Holographic Optical Elements for Optical Interconnection of Very Large Scale Integrated Circuits", Applied Optics, 26, 4377-4384.

3. Collier, R.J. et al., 1971, "Optical Holography", Academic Press, New York, USA.

4. Fuller, G., and Tarwater, D., 1986, "Analytic Geometry", Addison-Wesley Publ. Co., Massachusetts, USA.

5. Kostuk, R.K. et al., 1987, "Design Considerations For Holographic Optical Interconnects", Applied Optics, 26, 3947-3953.

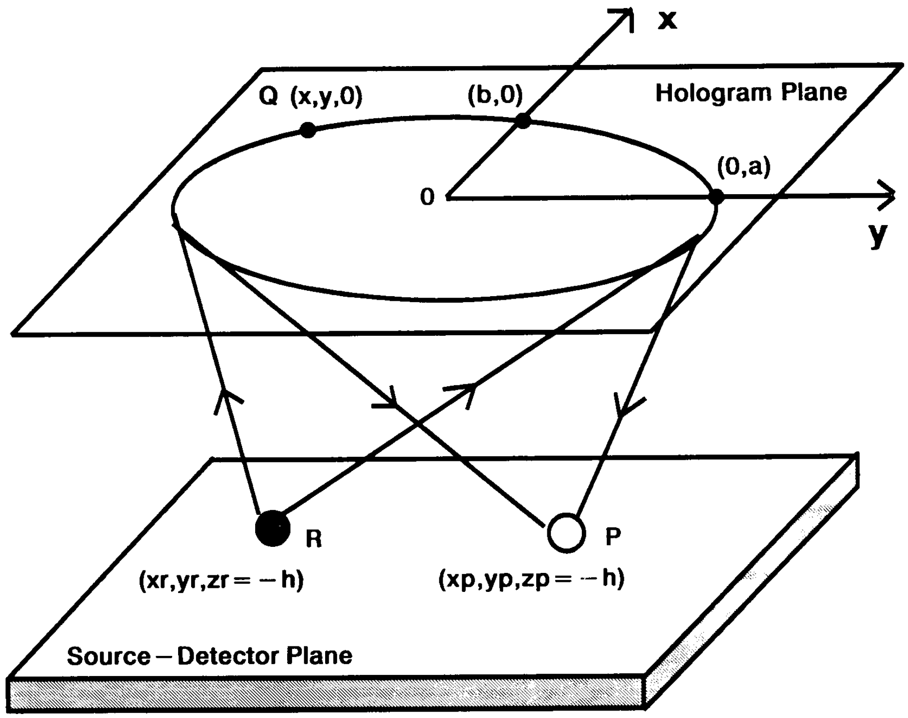

Figure 1 - System connecting one source to one detector

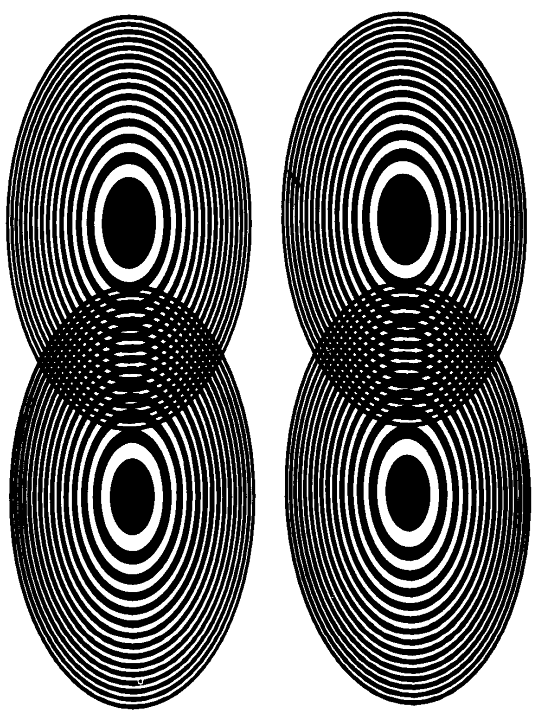

Figure 2 - HOE imaging one laser source to a 2 X 2 matrix of detectors.

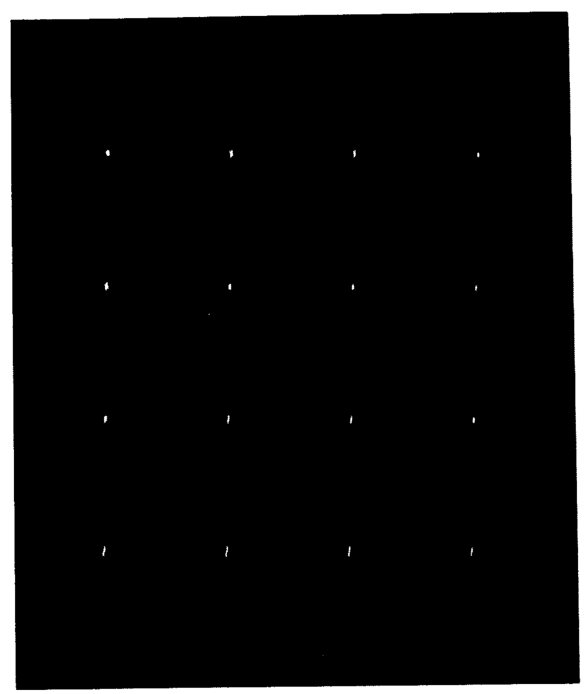

Figure 3 - Light spots at the detector plane produced by an HOE connecting one source to sixteen detectors.

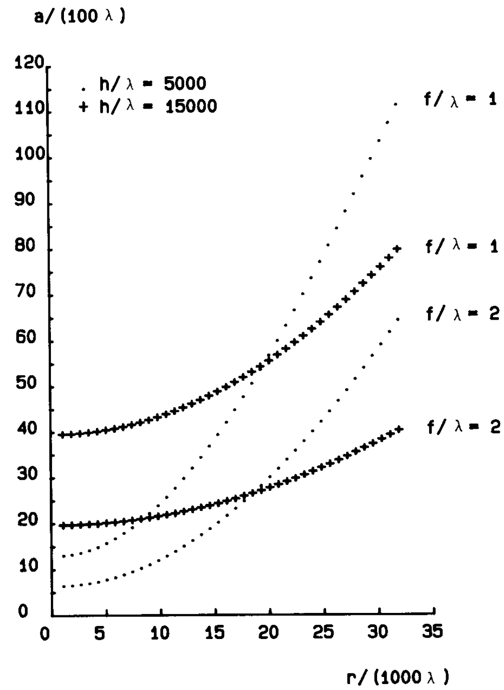

Figure 4 - (Major axis of ellipse)/2 vs. Distance between point sources for h = 5000λ and h = 15000λ.

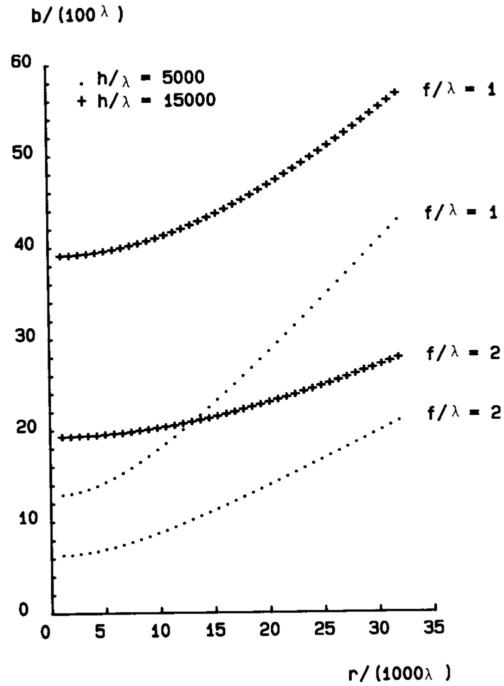

Figure 5 - (Minor axis of ellipse)/2 vs. Distance between point sources for h = 5000λ and h = 15000λ.

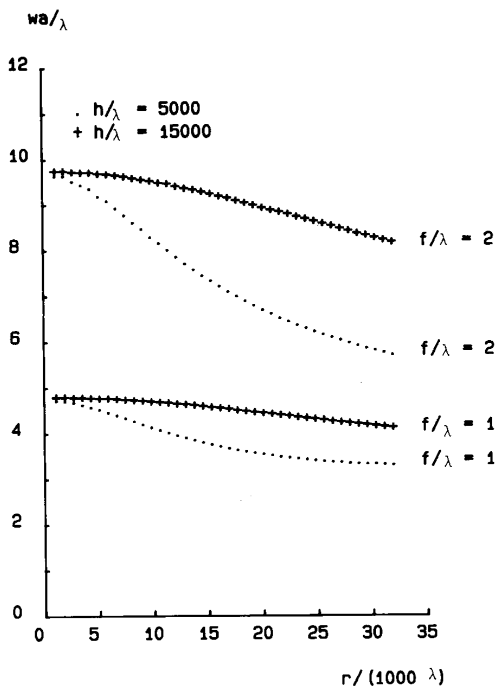

Figure 6 - Spot at the detector (wa) vs. Distance between point sources for h = 5000 λ and h = 15000 λ.

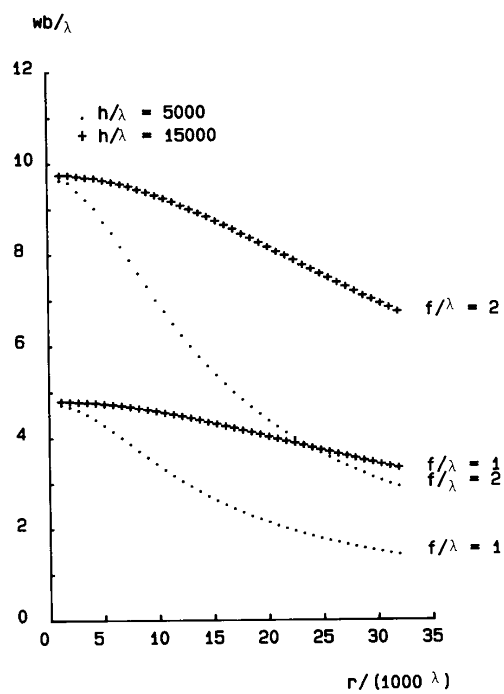

Figure 7 - Spot at the detector (wb) vs. Distance between point sources for h = 5000λ and h = 15000λ.